

Table S1

Table S1. Amino acid composition of the fingers, palm and thumb subdomains and the structural motifs in the different polymerases used for the study.

| | PV | CVB3 | HRV16 | FMDV |
|----------------------------------|-----------------------------------|-----------------------------------|-----------------------------------|-----------------------------------|
| <u>Subdomains</u> | | | | |
| Fingers | 1 – 68 96 – 190 269 – 286 | 1 – 68 96 – 190 271 – 287 | 1 – 68 96 – 190 269 – 285 | 1 – 66 97 – 195 280 – 296 |
| Palm | 69 – 95 191 – 268 287 – 380 | 69 – 95 191 – 270 288 – 381 | 69 – 95 191 – 268 286 – 379 | 67 – 96 196 – 279 297 – 392 |
| Thumb | 381 – 461 | 382 – 462 | 380 – 460 | 393 - 470 |
| <u>Motifs</u> | | | | |
| A | 229 – 240 | 229 – 240 | 229 – 240 | 236 – 247 |
| B | 293 – 312 | 294 – 313 | 292 – 311 | 303 – 322 |
| C | 322 – 335 | 323 – 336 | 321 – 334 | 332 – 345 |
| D | 338 – 362 | 339 – 363 | 337 – 361 | 348 – 373 |
| E | 363 – 380 | 364 – 381 | 362 – 379 | 374 – 392 |
| F | 153 – 178 | 153 – 178 | 153 – 178 | 158 – 183 |
| G | 113 – 120 | 113 – 120 | 113 – 120 | 114 - 121 |
| <u>Functional regions</u> | | | | |
| I | 107-112 | 107-112 | 107-112 | 108-113 |
| II | 184-200 | 184-200 | 184-200 | 189-205 |
| III | 405-420 | 406-421 | 404-419 | 416-430 |

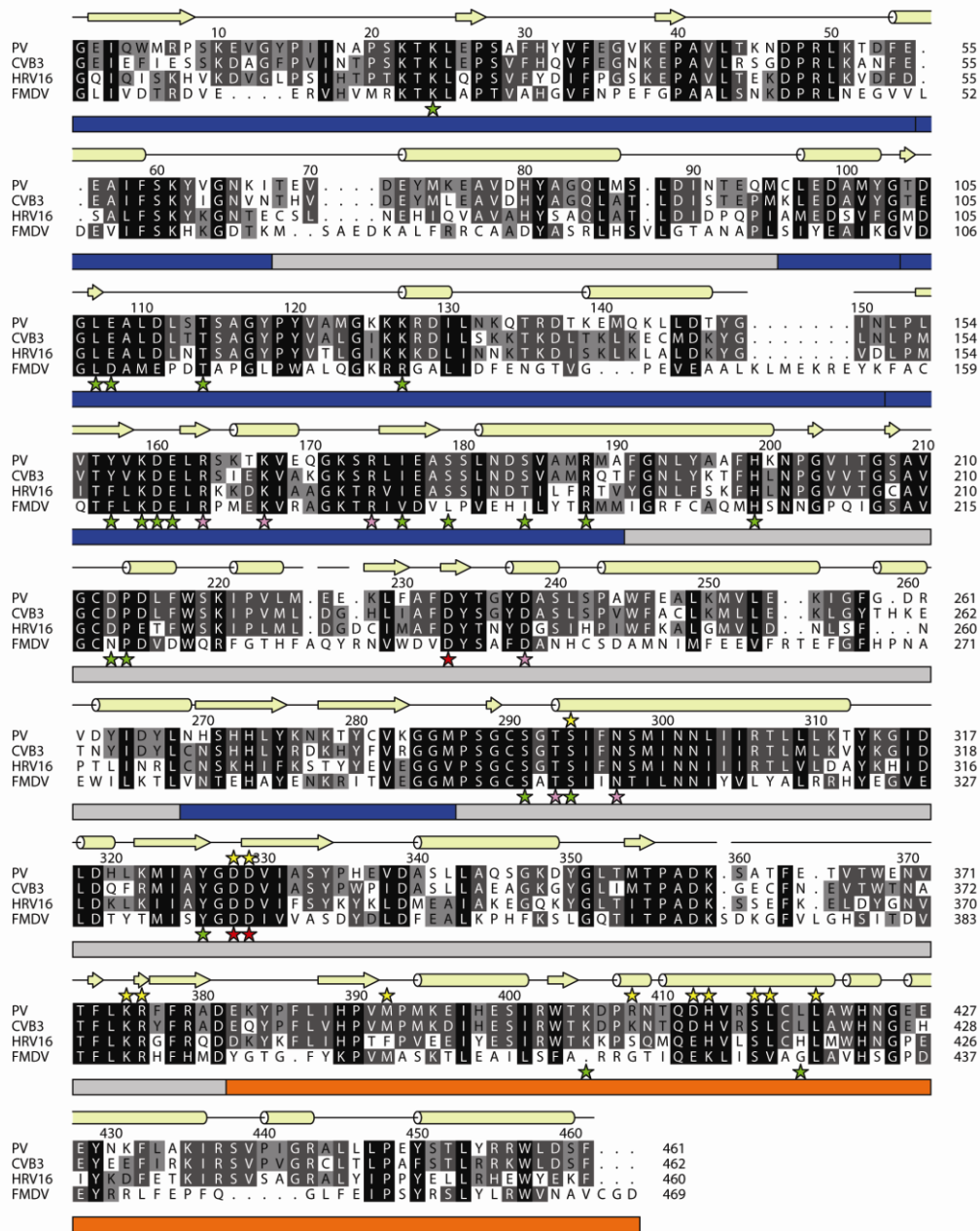


Figure S1. Structure-based sequence alignment of RdRps from: PV (PDB code 1RA6), CVB3 (3CDU), HRV16 (1XR7) and FMDV (1U09). The secondary structure for PV RdRp is shown at the top of the alignment. The colored bar at the bottom of the alignment highlights the different subdomains (fingers: blue; palm: grey; thumb: red). The alignment is shaded according to residue similarity: similar in all sequences (black); similar in three sequences (dark gray); and similar in two sequences (light gray). Residues critical for the polymerase function are marked by symbols at the top and bottom of the alignment: metal binding residues (red stars), nucleotide binding residues (magenta stars), template RNA binding residues (green stars), and primer RNA binding residues (yellow stars). The alignment was done using the program MUSTANG-0.3 [Konagurthu, A. S., Whisstock, J. C., Stuckey, P. J. & Lesk, A. M. (2006). MUSTANG: a multiple structural alignment algorithm. *Proteins* 64, 559-74]; the figure was prepared using ALINE [Bond, C. S. & Schuttelkopf, A. W. (2009). ALINE: a WYSIWYG protein-sequence alignment editor for publication-quality alignments. *Acta Crystallogr D Biol Crystallogr* 65, 510-2].

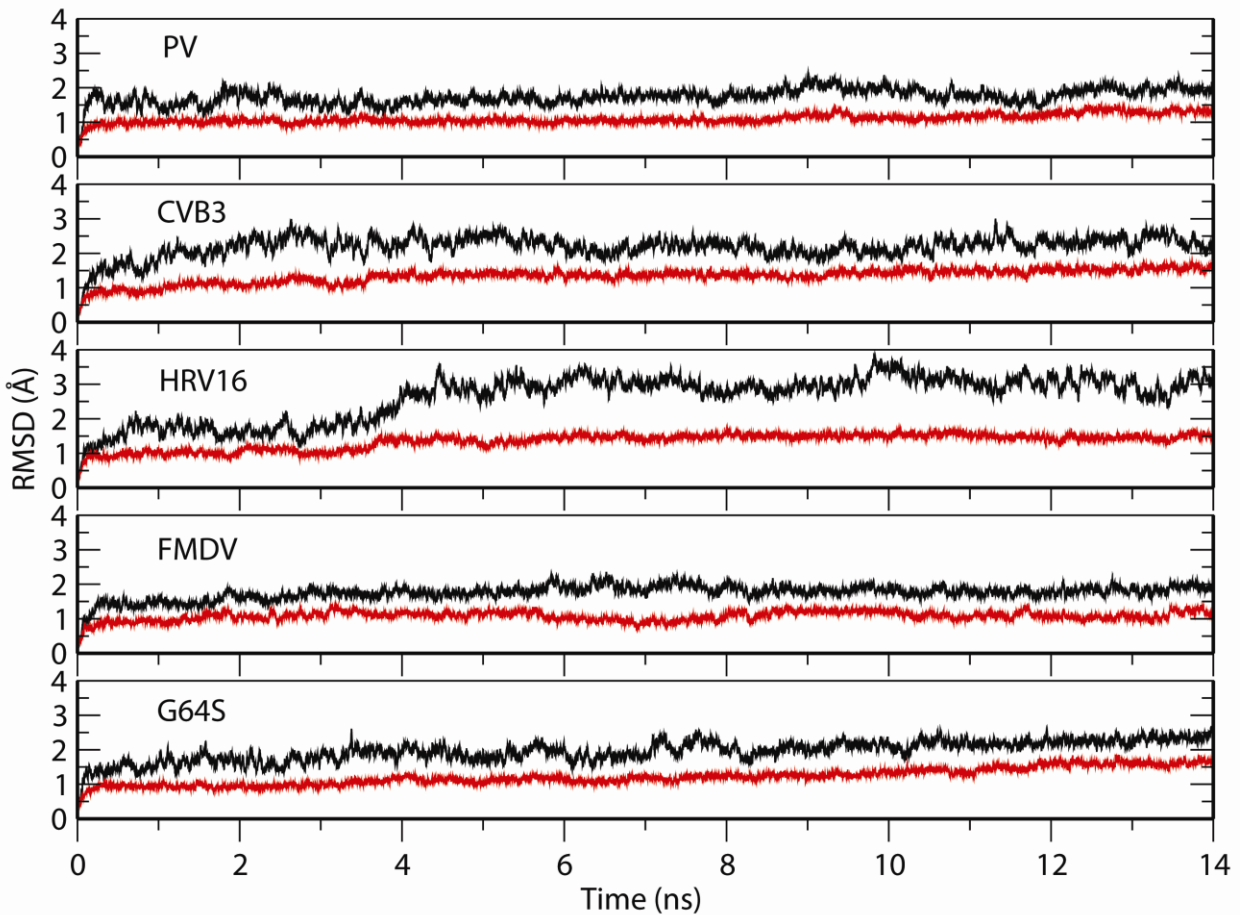


Figure S2. RMSD analysis revealed stabilization of the MD simulation trajectories 2 to 4 ns after the start of simulation. The root-mean square deviations (RMSD) for the backbone atoms are plotted for the different simulated polymerases. Before calculation, the trajectory structures were superimposed on the starting structure using all residues (black line) or palm residues (red line). The plot was used to determine the starting time for the production run: 2 ns (PV), 3 ns (G64S), or 4 ns (CVB3, HRV16 and FMDV). For PV, G64S, and FMDV the simulations continued for 25, 25 and 20 ns, respectively, without dramatic change in the RMSD.

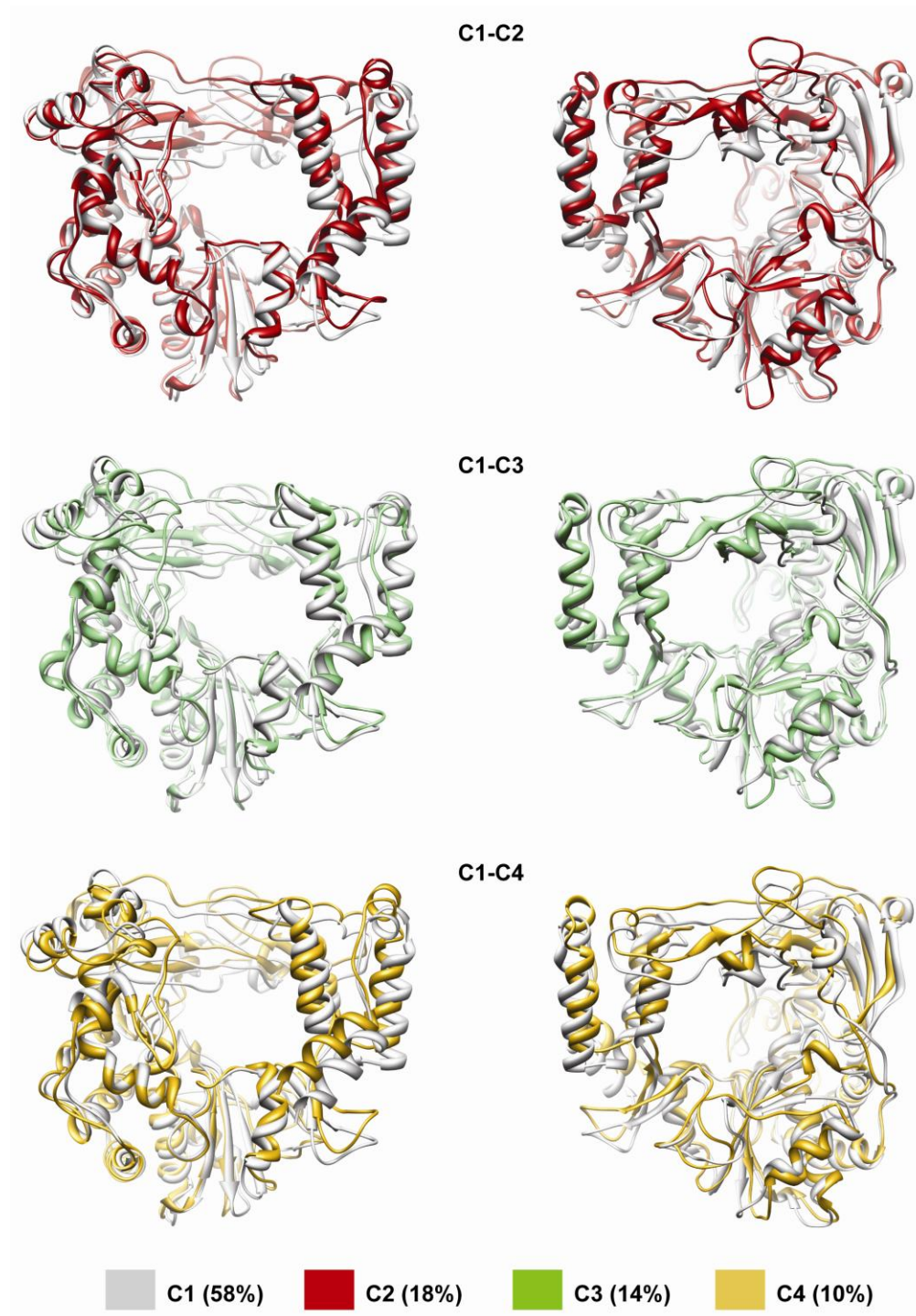


Figure S3. Cluster analysis of PV RdRp MD trajectory. Snapshots obtained from the PV RdRp simulation trajectory sampled at 10 ps interval (2,300 structures) were grouped into four clusters of different size. Representative structures from the clusters (C1-C4) are superimposed using C1 structure as a reference and shown in two views: left, looking through the RNA channel; right, looking through the NTP channel. The clusters are depicted in different colors. The color guide is shown at the lower right of the panel.

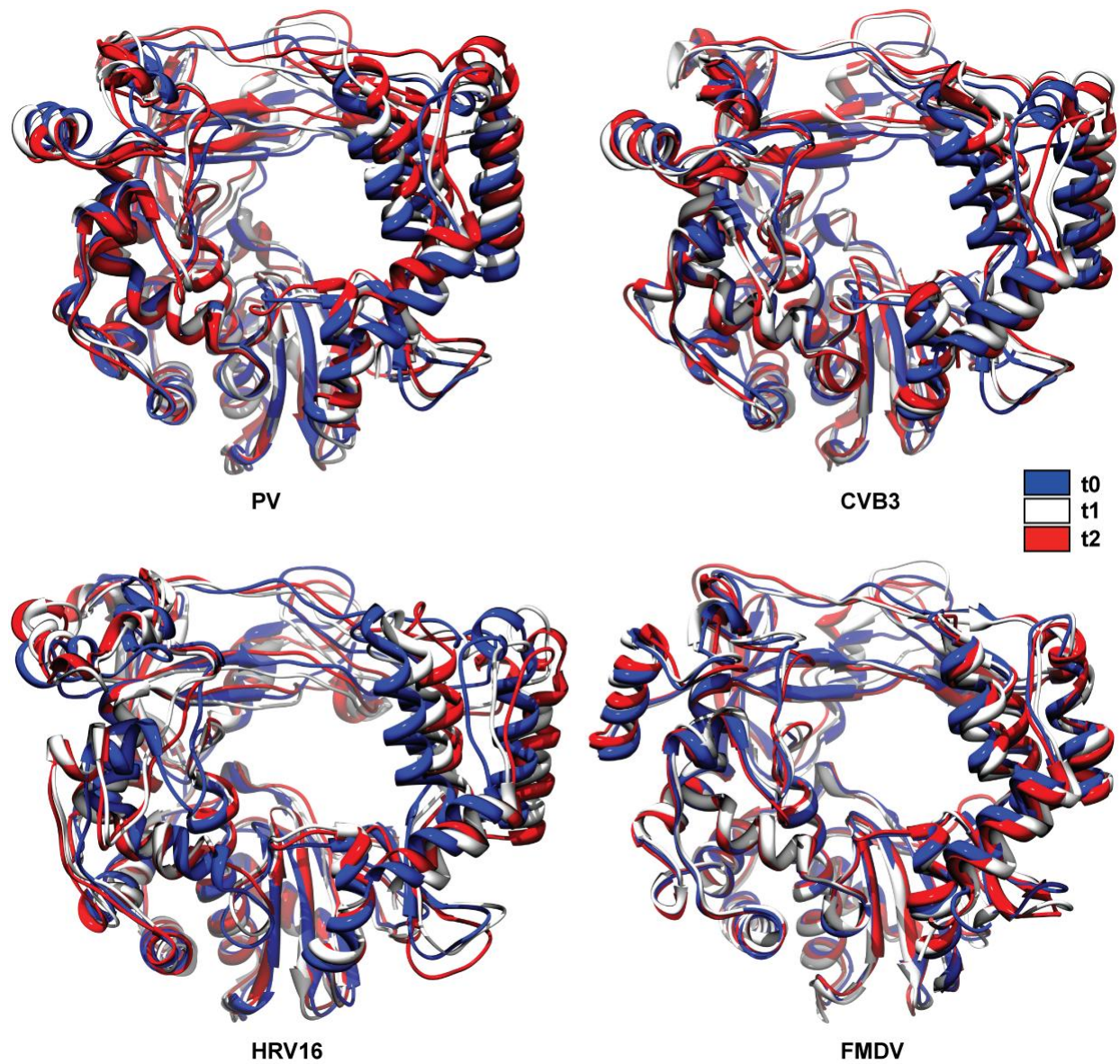


Figure S4. Snapshots from the MD simulations. Three snapshots from the simulated trajectories are shown for the different polymerases. The colored structures correspond to the beginning, middle and end of the trajectories.

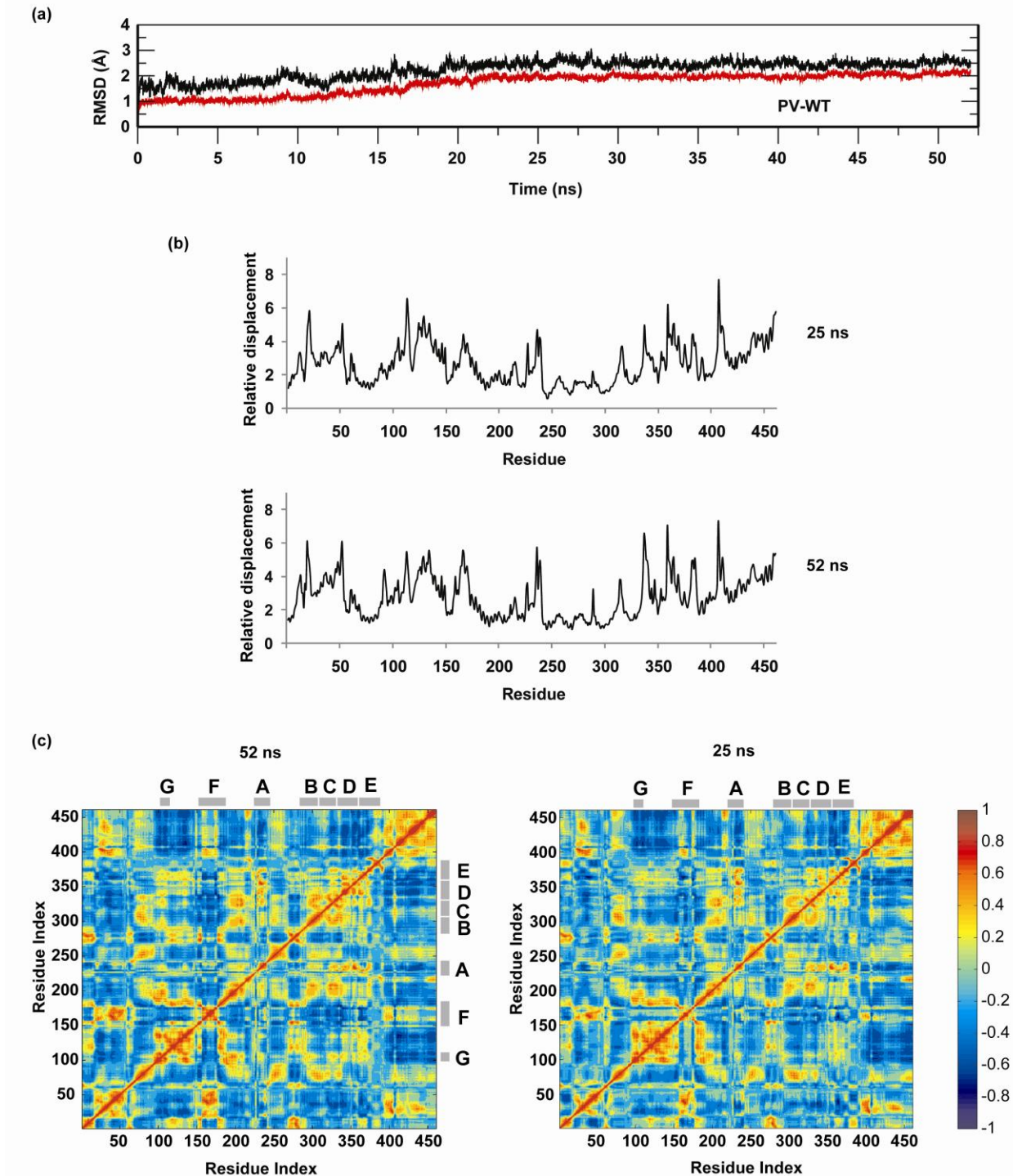


Figure S5. Comparison of 25 and 52 ns MD simulations of PV RdRp. (a) RMSD analysis of the 52 ns simulation. The rising in the RMSD between 12 and 20 ns is due to progressive conformational changes of motifs A, D and E as well as regions 256-261, 313-319, and 326-329 of the palm. (b) PCA analysis and (c) DCCM analysis of the production runs of the 25 and 52 ns MD simulations of PV RdRp produced similar results.

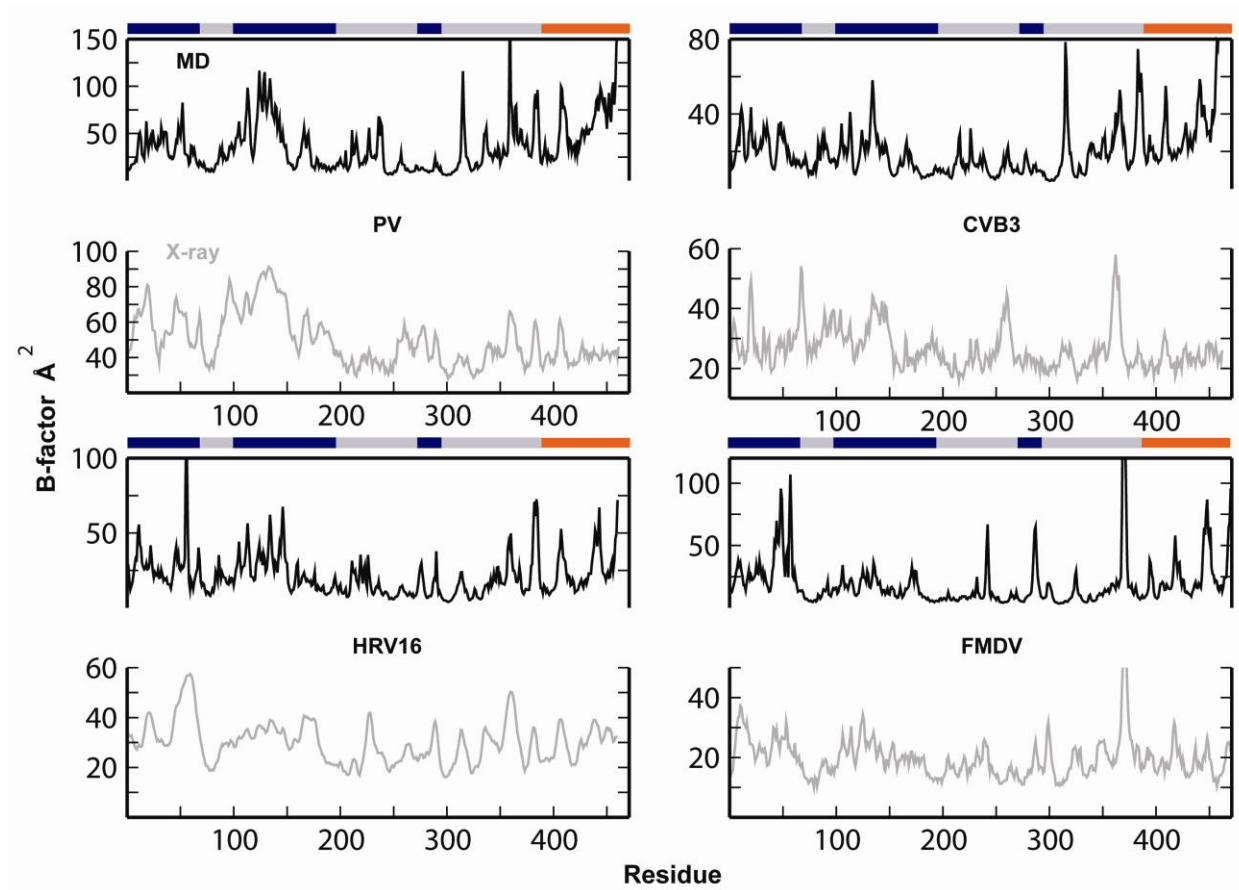


Figure S6. B-factor analysis of simulations of the different polymerases revealed dynamic regions not seen by X-ray diffraction. Plots of the B-factors averaged over the protein backbone atoms calculated from simulation (top, black line) and that from X-ray diffraction (bottom, grey line) are shown. Generally, the pattern of the calculated B-factor is in agreement, qualitatively, with that obtained from crystal structure. Regions that suffered from crystal contacts showed higher calculated B-factors compared to the crystal structure. The colored bars at the top mark the sequence regions corresponding to the fingers (blue), palm (grey) and thumb (red) subdomains in the different polymerases.

Figure S7

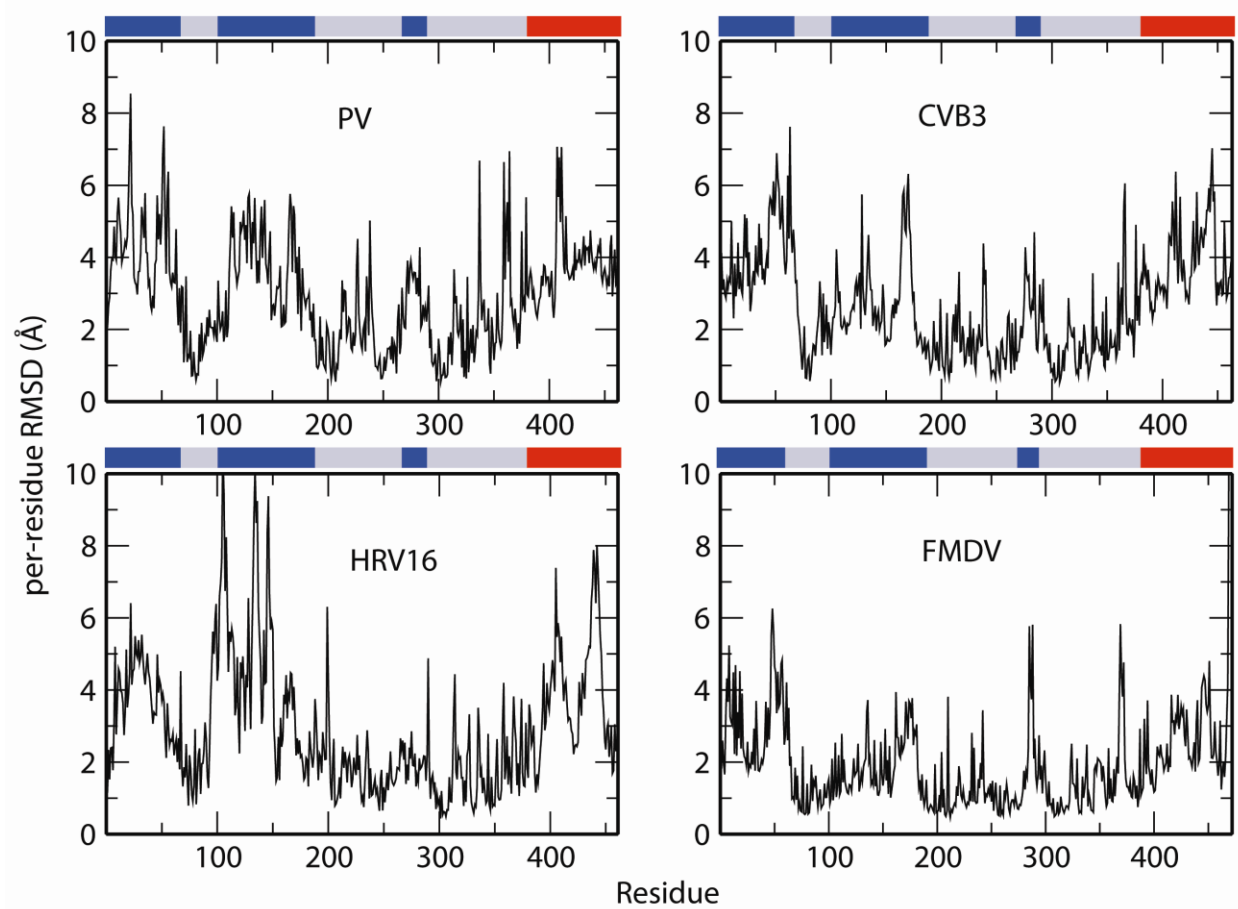


Figure S7. Per-residue RMSD analysis. The root-mean square deviations for the individual residues averaged over the last 10 ns of the simulation trajectories of RdRp from PV, CVB3, HRV16 and FMDV are shown. Before calculation, the structures of the MD trajectory were superimposed onto the minimized starting structure utilizing the backbone atoms of the palm subdomain. The high RMSD values of the fingers and thumb relative to the palm indicates conformational changes. The positions of the different subdomains are marked by the colored bars, using same colors as Figure S1, at the top of the plots.

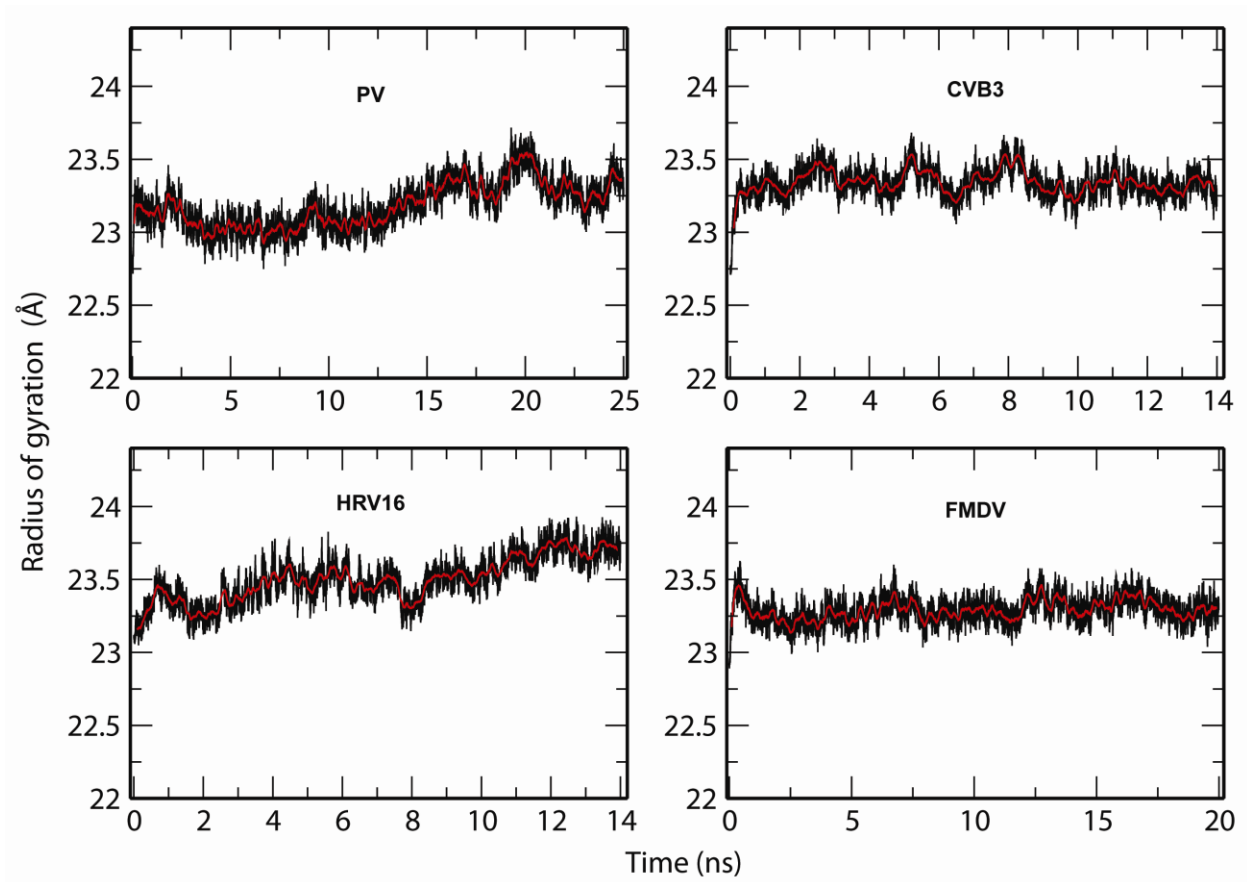


Figure S8. Radius of gyration analysis. The time evolution of the radius of gyration during the simulations of PV, CVB3, HRV16 and FMDV RdRps are shown. Initially, the radius of gyration increased and then continued to oscillate around average values. The changes in the radius of gyration observed during simulation correlates with changes between open and closed conformations of the enzymes shown in Figures 6 and S8.

Figure S9a

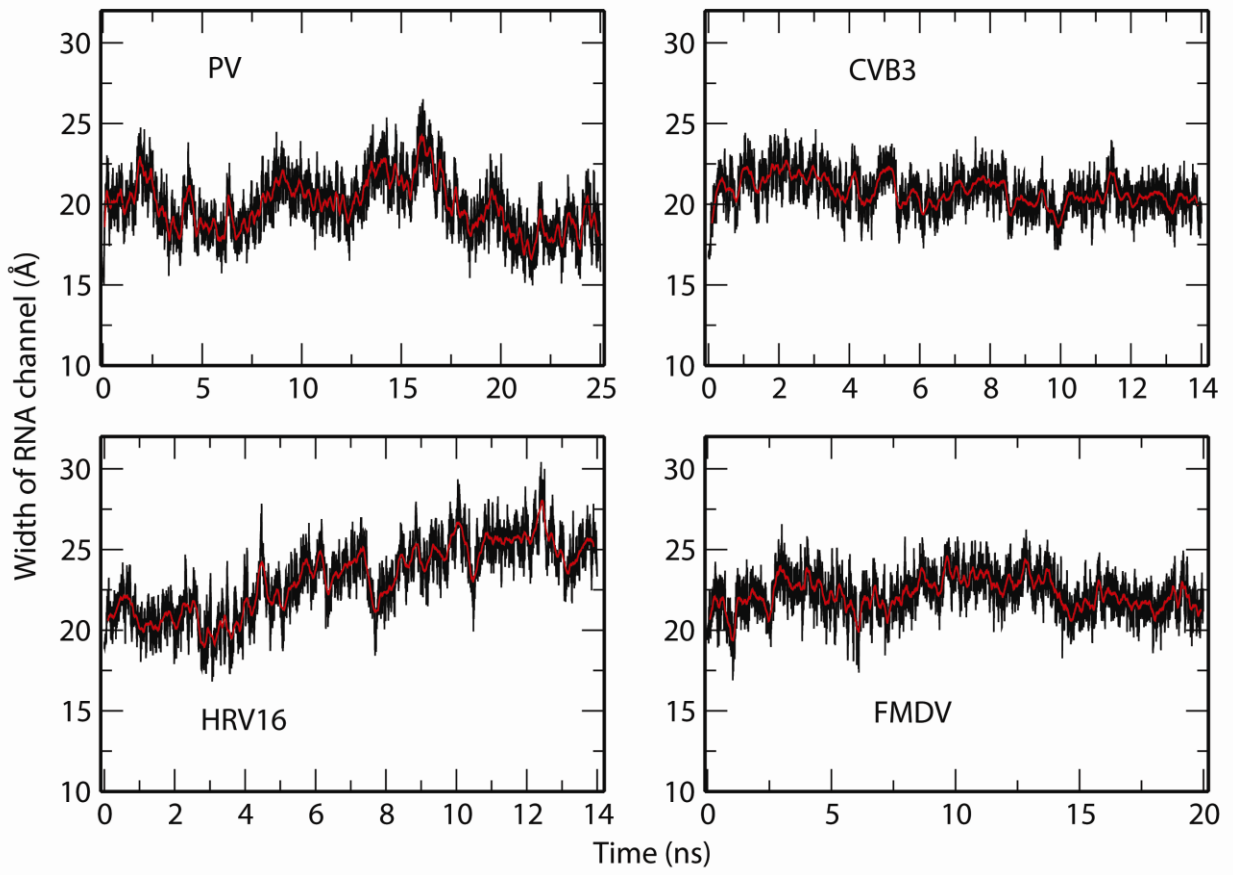


Figure S9b

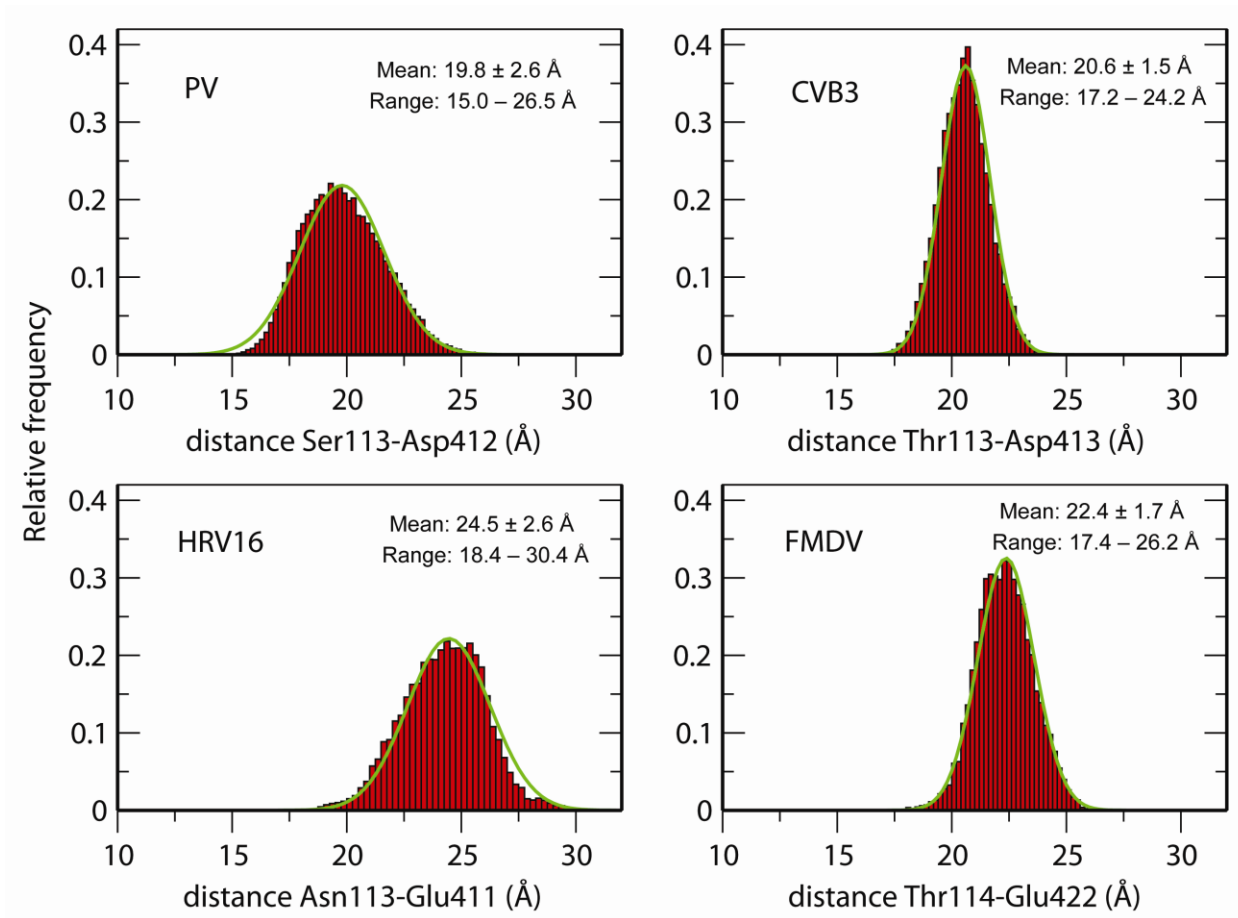


Figure S9. The RNA channel width as a probe for open/closed conformational change in RdRps. The width of the RNA entry channel in the polymerases from PV, CVB3, HRV16 and FMDV -- defined by C α -C α distance between two residues from the fingers and thumb at the mouth of the channel -- was probed during the simulations. (a) The time evolution (black line) and the running average, using 200 ps window, (red line) of the C α -C α distances between: Ser113-Asp412 (PV), Thr113-Asp413 (CVB3), Asn113-Glu411 (HRV16) and Thr114-Glu422 (FMDV) over the simulation course are shown. (b) The distributions of the distances shown in (a) along with the corresponding Gaussian fittings are shown. The parameters of the mean (obtained from the Gaussian fitting) and the range of the channel width are given at the top right of the plots.